Innovare Academic Sciences

International Journal of Pharmacy and Pharmaceutical Sciences

ISSN- 0975-1491 Vol 7, Issue 10, 2015

Original Article

TOPICAL GEL INCORPORATED WITH NON-IONIC SURFACTANT BASED SOLID LIPID MICROSPHERES OF KETOPROFEN: PHYSICOCHEMICAL ANALYSIS AND ANTI-INFLAMMATORY EVALUATION

RASHMI SAREEN[1,4], VARUN BHARDWAJ[2], VINEET MEHTA[3], ARUN SHARMA*[1,2]

[1]Department of Pharmaceutics, School of Pharmaceutical Sciences, Shoolini University, Bajhol, Solan, Himachal Pradesh 173229, India, [2]Department of Pharmacy, Jaypee University of Information Technology, Waknaghat, Solan, Himachal Pradesh 173234, India, [3]Institute of Pharmaceutical Sciences, Kurukshetra University, Kurukshetra Haryana, 136119, India, [4]School of Pharmacy, Bharat Institution of Technology, Meerut, Uttar. Pradesh, 250103 India

Email: mearun2010@yahoo.in

Received: 20 Jun 2015 Revised and Accepted: 08 Aug 2015

ABSTRACT

Objective: The present study was aimed at the fabrication and characterization of solid lipid based microspheres (SLM) of Ketoprofen (KPF) and comparing its anti-inflammatory potential with the marketed formulation.

Methods: Stearic acid as a lipid and tween 20, 80, span 20 and 80 as surfactants (at various concentrations) were utilized for formulation of topical delivery. Microparticles were successfully fabricated (0.71-3.12 µm) by hot melt microencapsulation technique and were characterised by photomicroscope, FTIR, scanning electron surface morphology, particle size analysis, zeta potential, fluorescent microscopy and *In-vitro* drug release studies followed by *In-vitro* and *In-vivo* anti-inflammatory studies.

Results: Results revealed that tween 80 resulted in exceptional KPF entrapment efficiency of 82.6% with spherical rough surface morphology. *In-vitro* drug release showed the initial burst release of 47% upto 2h followed by sustained release of 70% for 12h. By employing drug release kinetic modelling, formulations were found to obey Higuchi model and Korsmeyer-Peppas model. Further the *In-vitro* permeation study of optimized gel formulation represented better drug uptake through rat skin in comparison to marketed product. Finally, SLMs were found to possess superior *In-vitro* and *In-vivo* anti-inflammatory potentials when compared to marketed formulation.

Conclusion: SLMs proved to be promising drug carrier system for KPF topical delivery as they possessed the desirable particle size with high ability for drug entrapment with sustained anti-inflammatory effect.

Keywords: Ketoprofen, Solid lipid microsphere, Controlled release, Anti-inflammatory activity.

INTRODUCTION

Inflammation is a complex biological response of our body against external and internal stimuli such as; irritants, pathogens or damaged cells which results in irritation, redness, heat and pain [1, 2]. This may results in disability and loss of normal body function, as commonly seen in osteoarthritis and rheumatoid arthritis [3]. Ketoprofen (KPF) is the potent NSAID (non steroidal anti-inflammatory drug) which act as cyclooxygenase (COX) inhibitor. Therapeutically, it has been recommended for the treatment of typical arthritis or associated disorders as well as an effective anti-inflammatory, antipyretic and analgesic agent [4, 5]. However, oral administration of KPF showed less therapeutic concentration in the joint cavity, as it undergoes "first-pass" metabolism [6]. Additionally KPF is associated with sever gastrointestinal side effects which include ulceration, gastrointestinal perforation and bleeding [7]. Due to short half-life of KPF, the frequency of dose increases in order to maintain its therapeutic concentration [8] resulting in increased associated side effects. In this context, an appropriate topical controlled release dosage form can be a better alternative choice in order to deliver KPF directly to the affected area.

Topical delivery provides the suitable advantages to avoid the associated GIT side effects of an oral route as well as better patient compliance and bypasses first pass metabolism [9, 10]. In recent time, greater attentions have been devoted to polymeric based microparticles/microspheres and are widely investigated as suitable carriers for topical delivery [11]. Solid lipid microspheres (SLM) are well known for their advantageous properties such as biodegradability, physicochemical stability and higher hydrophobic drug molecule encapsulation efficiency [12, 13]. SLMs had shown exceptionally suitable for oral [14], pulmonary [15, 16] intramuscular and topical or subcutaneous delivery of drugs. Topical delivery possessed by SLMs is by virtue of their eminent affinity towards stratum corneum [17]. Moreover, non-ionic surfactants have been documented and utilized as those with the least toxicity and irritant index. These decisive properties make these agents as potential penetration enhancers in transdermal delivery systems [18].

In this present investigation, a SLM based drug delivery system of KPF for topical application was prepared and evaluated. In particular, we employed the non ionic surfactant, owing to its better spherical morphology for efficient drug release from the fabricated SLMs. Afterward physicochemical characterization of formulation was carried out in order to obtain optimised SLMs size and morphology with improved drug release profile. The best SLM formulation (Carbopol 934P based gel) was further subjected for *In-vitro* and *In-vivo* anti-inflammatory screening.

MATERIALS AND METHODS

Material

Ketoprofen (KPF) was obtained as a gift sample from Odian Health Care Pvt. Ltd. Solan, Himachal Pradesh (India). Carbopol 934P was provided by Qualikems Laboratory Reagents, Triethanolamine was purchased from Merck chemicals and carrageenan was purchased from Sigma Aldrich. Stearic acid, tween 20, tween 80, span 20 and span 80, potassium dihydrogen orthophosphate, sodium chloride and disodium hydrogen orthophosphate were purchased from Himedia. Methanol and ethanol absolute (purity>99.9%) was supplied by Merck Chemicals. Double distilled water was used for all experiments. All other reagents were of reagent grade and used as received without any purification.

Fabrication of SLM

SLMs were prepared by using hot melt microencapsulation technique (normal or phase inversion technique) with slight

modifications [19]. Briefly, stearic acid (lipid) was melted in a beaker at 70 °C. Weighed amount of KPF was dispersed in melted stearic acid under continuous stirring on magnetic stirrer to form hot melt mixture. Hot mixture was emulsified into an aqueous surfactant solution and was heated above lipid melting point to form oil/water emulsion. Four different surfactants (span 20, span 80, tween 20 and tween 80) were added in different concentrations as shown in table 1. The o/w emulsion was poured into 100 ml of ice-cooled aqueous phase (2 °C–5 °C) and finally allowed to cool. Microspheres were allowed to settle down and after 15 min aqueous phase were decanted, microspheres were filtered, washed thrice with deionised water and freeze dried using Lyophilisor (Allied Frost FD-3).

Physicochemical characterization

Light microscopy

Optical light microscopy was performed to visualize physical appearance of developed SLMs by using Olympus BX53 microscope at 20X and 100X magnification. Dried microspheres were placed on glass slide, glycerine drop was used to fix them onto the glass slide and the cover slip was placed on the top.

Fourier transform infrared spectroscopy (FTIR) analysis

FTIR spectra were determined (FTIR Instrument of Agilent Technologies 630 Cary) in order to investigate possible drug-excipient chemical interactions or compatibility between the moieties. Spectra were obtained by running Micro Lab software and interpretation was made.

Estimation of percent yield, drug loading and entrapment efficiency

Lyophilized SLMs from each formulation were weighed and respective percentage yield (PY) was calculated by using equation 1.

$$\text{PY} = \frac{\text{Mass of the obtained microspheres}}{\text{Initial mass of the drug+Initial mass of polymer}} \times 100 \quad \textbf{(1)}$$

Drug entrapment efficiency was determined by lysis of SLM with ethanol using sonicator (citizone-ultrasonic-Model-YJ5120). 50 mg of SLMs were weighed and dissolved in 10 ml of ethanol and further subjected to sonication for 15 min to get the clear transparent solution. By using UV visible spectrophotometer (Systronics-Model-2202), the concentration of KPF in ethanol was evaluated at 258 nm. Entrapment efficiency was determined for each batch in triplicate. Percentage entrapment efficiency (EE) and drug loading (DL) was calculated using equation 2 and 3.

$$\text{EE (\%)} = \frac{(\text{Total drug}) - (\text{Free drug})}{(\text{Total drug})} \times 100 \quad (2)$$

$$\text{DL (\%)} = \frac{(\text{Initial drug}) - (\text{Free drug})}{(\text{Mixed Lipid})} \times 100. \quad (3)$$

Particle size distribution

Beckman coulter Zeta sizer was used to determine particle size of various prepared microspheres. Lyophilized microspheres were first re-dispersed in de-ionised water and placed on the sampling rack. Type I-A dispersant was used to prevent the microsphere aggregation. Results provided are the average of triplicate analyses.

Morphology study

Surface morphology and shape of microscopes were observed by scanning electron microscopy (SEM-QUANTA 250, FEI Makers). Microspheres were mounted onto metal stubs using double-sided adhesive carbon conductive tap and placed inside the vacuum chamber. Moving electrons from tungsten filament were made incident to sample and surface morphology of SLMs was studied.

Drug distribution inside the SLM

Fluorescence microscopy (OLYPMUS BX53) was used to study distribution and internal, localization of drug into the matrix system of microspheres. For this, fluorescent Rhodamine B dye was selected and the same fabrication technique was used to develop Rhodamine B loaded SLMs. Rhodamine B was excited via a mercury lamp (550 nm band pass filter) and images were captured by using Image pro plus software.

***In vitro* release of KPF from SLM**

In vitro drug release from fabricated SLMs was determined by applying membrane diffusion technique (Franz diffusion cell) and using molecular porous membrane (Spectra/Por dialysis membrane 12–14.000). Microspheres, equivalent to 10 mg of KPF, were suspended in 5 ml phosphate buffered saline (pH 7.4) and placed inside the conical flask having 100 ml of PBS as the dissolution medium. Apparatus was adjusted at constant speed (50 rpm) and temperature of 32 °C. Samples were collected after 15 min, 30 min, 1, 2, 3, 4 h respectively and for every successive 2 h over a period of 12 h and assayed spectro-photometrically (Systronics-Model-2202) at 258 nm. Release data was further subjected to mathematic modelling to determine the release profile.

Mathematical modelling and drug release kinetics

Data from *in vitro* drug release were fitted to kinetic equations to describe the mechanism of drug release from microspheres. The employed kinetic models were zero-order equation, first-order equation, Higuchian and Korsmeyer–Peppas. Zero-order kinetics (eq. 4) depicts the linear relationship in between the released drug and time. First-order Kinetics (eq. 5) shows the correlation between the release amount of drug and the remaining drug to be released. Higuchi model [20, 21] gives the expression for the released drug which depends on the square root time (eq. 6). Rate constants for the respective models were calculated and to check out the further drug release mechanism, initial 60% of drug release were fitted in Korsmeyer–Peppas [22] models represented in equation 7.

$$Q_t = k0t \quad (4)$$

$$\ln Q_t = \ln Q_{\alpha +} k_1 t \quad (5)$$

$$Q_t = k_H t^{1/2} \quad (6)$$

$$Q_t = k_k t^n \quad (7)$$

Here Q_t is the released amount of drug at time t, Q_α is initial amount of drug, were as k_0, k_1, k_h and k_k are the corresponding release rate constants for zero-order, first-order Higuchian and Korsmeyer-Peppas model respectively and n is diffusion exponent for Korsmeyer-Peppas.

Preparation of ketoprofen loaded SLMs gel

Dispersion method was used for preparation of KPF-SLMs gel. KPF encapsulated SLMs were incorporated into a gel base of Carbopol 934P. Briefly, the gel was made by dispersing SLMs of KPF into 1% Carbopol 934P gelling solution to obtain 2.5% (w/w) gel under constant stirring. Few drops of triethanolamine were added as viscosity modifier or controller.

Characterization of SLM gel

pH, viscosity and spreadability

The pH of prepared gel was measured using a digital pH meter (Systronics instruments, India). Gel viscosity via rotating measurement was determined by using Brookfield DV III ultra V 6.0 RV cone and plate viscometer (Brookfield Engineering Laboratories, Middle-boro, MA) at 25+0.3 °C. Spreadability of prepared gels was determined by glass slide apparatus. Briefly, 10 grams of weight was attached to an upper slide and a thin layer of gel was placed in between the two slides, afterwards the time taken to separate completely one slide from other was noted [23].

Spreadability was then calculated by using the formula represented in equation 8.

$$S = \frac{M \times L}{T} \quad \ldots\ldots\ldots\ldots (8)$$

Where S is spreadability, M is the weight tide to upper slide, L is the length of glass slide, T as the time taken to separate slide completely from each other respectively.

Preparation of skin for *In-vitro* permeation studies

Rat abdominal skin was used for *In-vitro* permeation studies. Depilatory (hair removing cream) was applied on abdominal portion

of rat and hairs were completely removed from the skin. Afterward, abdominal skin was excised from rat with the help of the scalpel and fatty layer was removed by keeping skin in warm water at 60 °C. After 2 min, fatty layer was peeled off gently and skin was thoroughly washed with water and kept for saturation in phosphate buffer saline (pH 7.4) for 30 min.

***In-vitro* skin permeation study of SLM gel**

In-vitro comparison studies were performed via investigating permeation of KPF-loaded-SLMs Gel and marketed KPF gel (Fastum-Gel, India). The prepared skin was mounted on receptor compartment of modified Franz-diffusion cell with cross-sectional area of 3.91 cm^2. Receptor compartment was filled with 42 ml of degassed phosphate buffer (pH-7.4) maintained at 37±0.5 °C with constant stirring at 50 rpm. Prior to application of formulations, skin was allowed to equilibrate according to conditions for 1 h. Formulated gel and marketed gel of KPF (2.5%) were applied uniformly on dorsal side of the skin. Aliquots of 2 ml were withdrawn periodically and replaced with the same amount of saline solution to maintain receptor phase volume at a constant level. Collected samples were quantified spectro-photometrically at a wavelength of 258 nm and all recording was made in triplicates. Steady state flux was calculate from slope of the plot using regression analysis [24] and permeability co-efficient (Kp) of the drug from membrane was calculated using equation 9.

$$\text{Permeability co-efficient} = \frac{\text{steady} - \text{state flux}}{\text{drug Initial concentration in donner compartment}} \quad \ldots\ldots\ldots\ldots\ldots(9)$$

***In-vitro* evaluation of anti-inflammatory activity**

Inhibition of albumin denaturation

Method from Mizushima *et al.*, [25] was used for the evaluation of *In-vitro* anti-inflammatory activity of SLM-loaded-KPF-Gel and marketed formulation with slight modifications. Briefly, 1 ml sample solution was withdrawn during *In-vitro* drug release study at 0, 0.5, 1, 2, 4, 6, 8, 10 and 12 h, thereafter, subjected to *In-vitro* anti-inflammatory analysis. For the purpose of control, equal volume of distilled water was used. To each reaction mixture, 1 ml of bovine albumin (1% in distilled water) was transferred and pH was adjusted to 6.3 by using small amount of 1N HCl. Samples were incubated for 30 min at 37 °C in the dark followed by incubation at 57 °C for 5 min. Reaction tubes were then cooled under running tap water and turbidity of all the samples were recorded spectro-photometrically (Systronics-Model-2202) in triplicate at 660 nm. Percentage inhibition of albumin denaturation was calculated by using equation 10.

$$\text{Percentage inhibition} = \frac{\text{Abs Control} - \text{Abs Sample}}{\text{Abs Control}} \times 100 \quad \ldots\ldots\ldots\ldots (10)$$

RBC membrane stabilization

Preparation of red blood cells (RBCs) suspension

Sufficient amount of fresh rat blood was collected in the glass tube having 1.8 mg/ml 5% EDTA solution and mixed gently. Blood sample was centrifuged at 3000 rpm for 15 min and washed thrice with equal volume of normal saline. 10% v/v suspension of RBC was prepared in normal saline. Suspension was stored at 4 °C and used within 6 h of preparation [26, 27].

RBC membrane stabilization method

Reaction mixture consisted of 1 ml phosphate buffer, 2 ml hypo-saline (0.36 %), 0.5 ml blood suspension and 1 ml of sample taken from *In-vitro* release study at 0, 0.5, 1, 2, 4, 6, 8, 10 and 12h respectively. Reaction mixture was incubated at 37 °C for 30 min, followed by centrifugation at 3000 rpm for 20 min. Collected supernatant was then subjected to spectrophotometric analysis at 560 nm [28]. All the readings were taken in triplicate and percentage membrane stabilization was calculated by using equation 11.

$$\text{Percentage membrane stabilization} = \frac{\text{Abs Control} - \text{Abs Sample}}{\text{Abs Control}} \times 100 \quad \ldots\ldots\ldots\ldots (11)$$

***In-vivo* anti-inflammatory study**

In-vivo anti-inflammatory activity of selected SLM formulation was studied by carrageenan induced paw edema in male Wistar rats and was compared to marketed formulation. All the experiments were performed according to CPCSEA guideline and approval from Institutional animal Ethics Committee (IAEC/SU-PHAR/13/007).

Animals weighing 130-150 g were divided into three groups and each containing five animals. Group I received a topical plane hydrogel, group II received marketed KPF-Gel and group III received SLM-loaded-KPF-Gel. 0.1 ml carrageenan solution (1% w/v in saline) was injected into sub-planter region of left hind paw of the rat and paw volume was measured after 0, 1, 2, 3, 4, 5, 6, and 12 h using plethysmometer. The edema rate and inhibition rate of each group were calculated by assigning equation 12 and13.

$$\text{Edema Rate (E\%)} = \frac{\text{Vt} - \text{Vo}}{\text{Vo}} \times 100 \quad \ldots\ldots\ldots\ldots (12)$$

$$\text{Inhibition Rate (I\%)} = \frac{\text{Ec} - \text{Et}}{\text{Et}} \times 100 \quad \ldots\ldots\ldots\ldots (13)$$

Where Vo is the mean paw volume before carrageenan injection (ml), Vt is the mean paw volume at different time internal (ml), Ec is the edema rate of control group, and Et is the edema rate of the treated group.

RESULTS AND DISCUSSION

Optical microscopy

Fig. 1 represents the optical microscopic images of drug loaded and blank microspheres revealing the spherical shape, discrete and uniform microspheres with negligible aggregation. Fig. 1 (a, c) depict the blank microspheres, whilst Fig. 1 (b, d) present the microscopic image of drug loaded microspheres at 20X and 100X magnification respectively.

FTIR analysis

Drug-excipient interactions were studied by FTIR spectral analysis. FTIR spectroscopy confirms the structural stability of KPF inside microspheres and compatibility between drug and stearic acid. FTIR spectra of pure drug, stearic acid and KPF-loaded-SLMs are presented in fig. 2. FTIR spectrum of stearic acid (fig. 2a) showed prominent band at 1700 cm^{-1} corresponding to C=O (stretching) and peaks at 2916 cm^{-1} and 2849 cm^{-1} were corresponded to–CH-bond having saturated carbon atoms. FTIR of KPF (fig. 2b) showed band of C=O stretching at 1695 cm^{-1}, aromatic C=O stretching at ~ 1655 cm^{-1} and 1595 cm^{-1},-CH-deformation of aromatic ring ~ 860 cm^{-1} and 690 cm^{-1}. These representative bands of KPF appeared with substantial compatibility of KPF-loaded-SLMs (fig. 2c) revealing that KPF is stable within SLMs without any kind of chemical interaction.

Percentage yield (PY), drug loading (DL) and percentage entrapment efficiency (EE)

PY, DL and EE of all the batches of KPF-loaded SLMs were performed in triplet and the corresponding values have been listed in table 2. PY values were found within the range of 73% to 91% respectively. It was observed that EE increases with increase in concentration of stabilizer, i.e. from 0.5 ml to 1.5 ml irrespective of surfactant type used. Interestingly, with the increase in surfactant concentration, solubility of drug inside lipid was enhanced. Similar results were obtained with other stabilizers. Formulations showed EE value ranging between 39.04%-82.61% (table 2) and highest entrapment efficiency was found to be with Tween 80 (F4; 82.61%). Formulations comprising span showed comparatively lower EE to others, moreover span 80 depict lower most EE compared to span 20. This can be explained in context to higher HLB value for span 20 than span 80. In case of tween, HLB does not play a major role as it is dominated by the stability of an emulsion system and it was found that tween 80 gives the more stable emulsion system in comparison to tween 20. In addition, the stability was observed for 30 d, where tween 80 was found better without any kind of clump formation and phase inversion. Hence the entrapment efficiency of different formulations were observed in following order; tween 80>tween 20>span 20>span 80, respectively. Similarly, DL also represents the

same pattern, with increase in amount of surfactant volume; DL also increases and varies from 38 % to 21 % (table 2). Based on the highest EE, four different formulations from each surfactant class (F1, F4, F7 and F10) were selected and subjected for further studies.

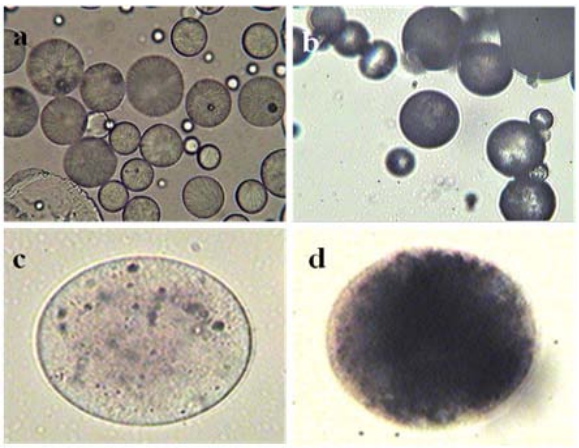

Fig. 1: Optical microscopic images of solid lipid microspheres; (a) blank SLMs in bulk, (b) drug loaded SLMs in bulk, (c) individual blank microsphere and (d) individual drug loaded microsphere. The images (a-b) are at 20X and (c-d) at 100X magnification

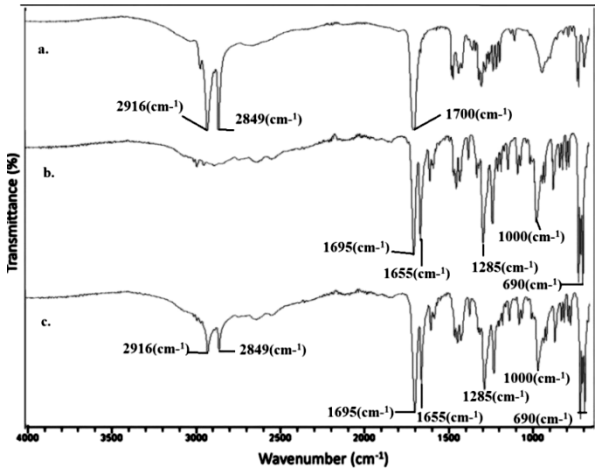

Fig. 2: FTIR spectrum of (a) stearic acid, (b) pure drug and (c) KPF-Loaded-SLMs

Surface morphology and particle size

Based on entrapment efficiency, scrutinized formulations (F1, F4, F7 and F10) were evaluated for surface morphology and particle size distribution. Fig.3 display the representative SEM of selected SLMs and it clearly shows that formulations have spherical morphology with rough surface (scale bar = 50 µm). Selected formulations were further investigated for particle size distribution and corresponding curve for subjected formulations F1, F4, F7 and F10 has been presented in fig. 3a, b, c and d, respectively.

Size distribution for all formulations was found in narrow range between 3.12±0.47 µm to 0.71±0.21 µm (fig. 3) suggesting them to be a suitable candidate for the topical route. Escribano and co-workers reported that the particle size less than 3 µm gets randomly distributed in stratum corneum and penetrates skin easily [29]. Polydispersity Index (PDI) values were found to vary from 0.293±*0.18* to 0.533±0.06 (table 3) depicting uniformity in the particle size distribution.

Drug distribution

Rhodamine B fluorescent dye was used for drug distribution analysis. When light of the particular wavelength from mercury lamp (550 nm band pass filter) made incident to surface of the dye loaded microspheres, dye molecules absorbs light, gets excited and emit light for longer duration. This emitted light was being captured and visualized as coloured particles. Fig. 4 represents fluorescence images of microspheres displaying drug distribution inside the matrix of SLM. Fig. 4a shows SLM-loaded-Rhodamine B under bright field mode. Colour distribution of dye inside the sphere is attributed to uniform distribution of drug (identified by the intense red colour). It was observed that dye was well encapsulated and distributed up to the core of the microsphere (fig. 4 b, c).

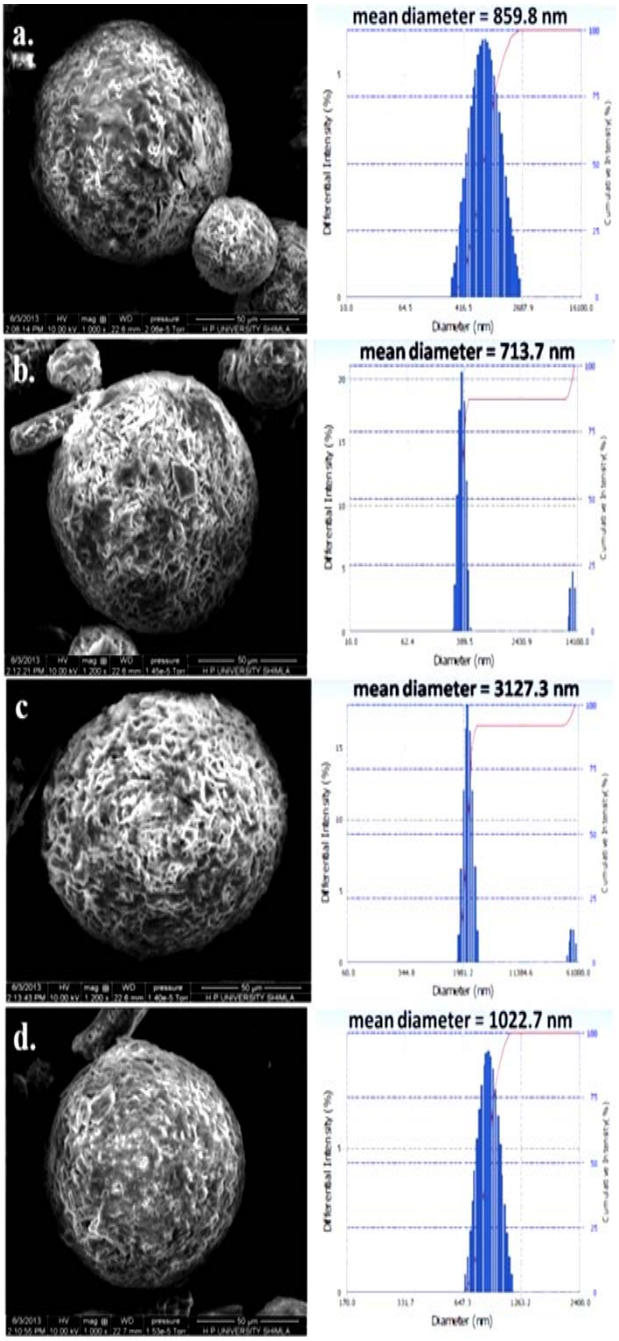

Fig. 3: SEM micrographs and corresponding diameter distribution histogram of SLMs; (a) F1-Tween 20 (1.5 ml), (b) F4-Tween 80 (1.5 ml), (c) F7-Span 20 (1.5 ml) and (d) F10-Span 80 (1.5 ml). All scales (a-d) are 50 µm respectively

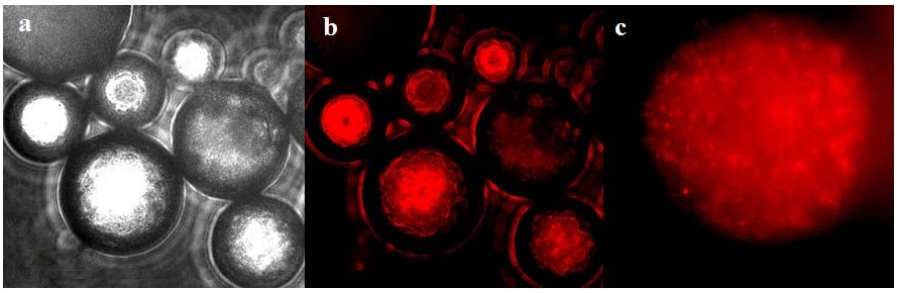

Fig. 4: Fluorescence micrographs represent the distribution of dye into the premises of Rhodamine–loaded SLMs; (a) Bright field showing microspheres in bulk, (b) Fluorescent image of microspheres in bulk and (c) individual microsphere. The images in (a), (b) are at 20X and (c) at 100X magnification

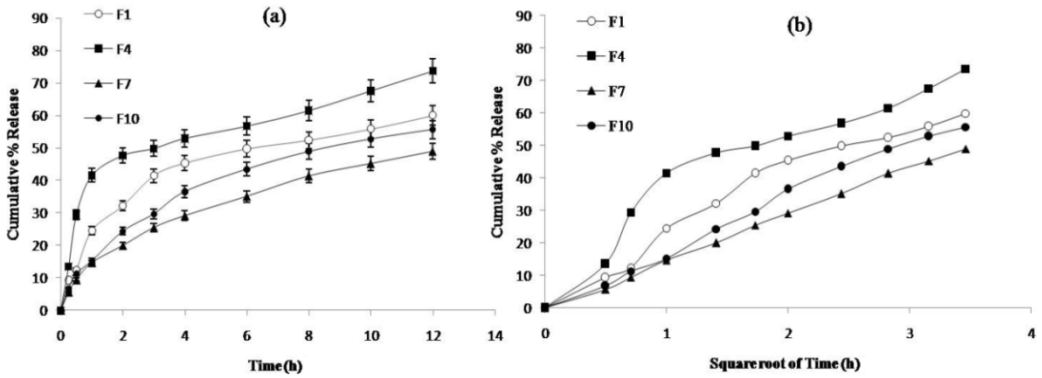

Fig. 5: *In-vitro* release profiles for; (a) the optimised formulation of KPF-loaded SLMs and (b) Higuchi kinetics release profile of KPF-loaded SLMs

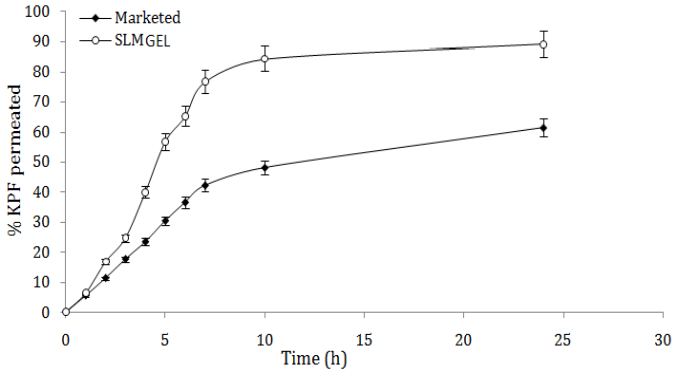

Fig. 6: The Comparative permeation profile of drug for KPF-loaded SLMs gel and marketed gel

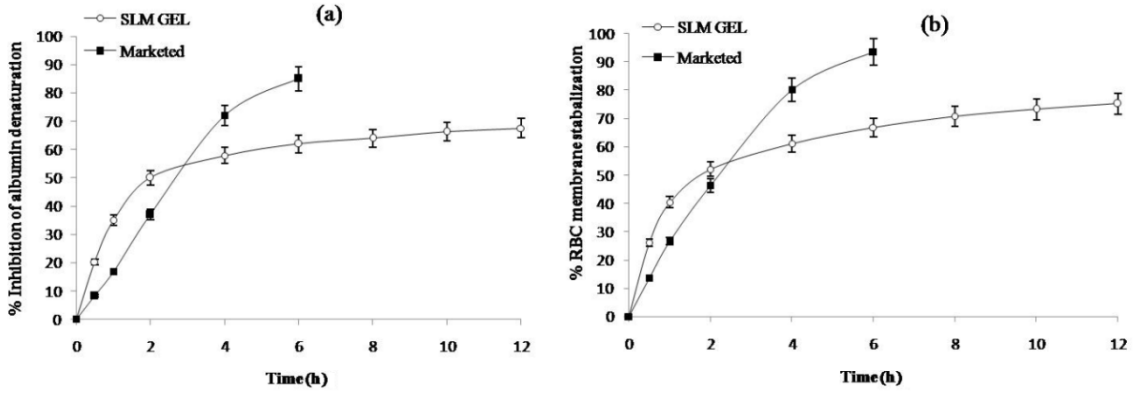

Fig. 7: *In-vitro* % inhibition of albumin denaturation by marketed product (a) SLM-loaded KPF gel and (b) *In-vitro* % RBC membrane stabilization profile of marketed product and SLM-loaded KPF gel

***In-vitro* release study of KPF from SLMs**

Percent cumulative *In-vitro* release of KPF for F1, F4, F7 and F10 has been depicted in fig. 5a. Selected formulations showed an initial burst release of 33-47 % (of total drug) within 2h followed by a slow and steady release of KPF up to 12h. Initial burst release of drug from microspheres is due to loosely associated drug molecules embedded in the surface layer of microspheres. Surface-associated drugs molecules are widely known to be the main cause for the initial burst release. Among all studied formulations, highest cumulative release was obtained for F4 approximately 70% within 12 h (1.5 ml Tween 80 as stabilizer).

Further, to gain better understanding of the release mechanism, *In-vitro* release kinetics (mathematic modelling) was applied. Release constants were calculated from the slope of appropriate plots and regression coefficient (R^2) were determined by linear regression analysis. First order release data of formulations was found in a range of 0.388-0.564 and 0.726-0.921 for zero order respectively (table 4). The release regression values (correlation coefficient values) were best fit within Higuchi plot (0.901-0.998) in comparison to first and zero orders (table 4). Thus, the drug release of KPF was found to be proportional to square root of time, suggesting that all formulations followed diffusion controlled release mechanism (fig. 5b). Similarly, drug release mechanism was also studied by applying Korsmeyer-Peppas model and exponent values were found to lie between 0.249-0.360. The *n* values were found to be less than 0.5 indicating Fickian release (table 4).

From the results, it was found that formulation F1, F4, F7 and F10 have the highest EE and particle size ranges between 0.7±0.21–3.1±0.47 µm, but amongst four formulations F4 was found to have narrow particle size distribution, and lowest PDI. In addition, EE of F4 was found to be 82.61 %, whereas for F1, F7 and F10 were 61%, 57.72% and 53.42%, respectively. The *In-vitro* release profile of F4 was found to be much controlled in comparison to other formulations. Therefore, formulation F4 was chosen for further investigation.

Table 1: Composition of anti-inflammatory KPF microspheres

Formulation code	F1	F2	F3	F4	F5	F6	F7	F8	F9	F10	F11	F12
Ketoprofen (mg)	400	400	400	400	400	400	400	400	400	400	400	400
Stearic acid (g)	2	2	2	2	2	2	2	2	2	2	2	2
Tween 20 (ml)	1.5	1	0.5	----	----	----	----	----	----	----	----	----
Tween 80 (ml)	----	----	----	1.5	1	0.5	----	----	----	----	----	----
Span 20 (ml)	----	----	----	----	----	----	1.5	1	0.5	----	----	----
Span80 (ml)	----	----	----	----	----	----	----	----	----	1.5	1	0.5

Table 2: Percentage yield, entrapment efficiency, drug loading within prepared SLM

Formulation code	PY (%)	DL (%)	EE (%)
F1	73.52+0.32	35.42±0.25	61.45+0.72
F2	79.30+0.41	28.61+0.18	56.26+0.22
F3	84.50+0.34	24.53+0.27	47.07±0.37
F4	87.58+0.52	38.48±0.31	82.61+0.73
F5	91.90+0.24	32.72+0.22	79.53+0.33
F6	83.41+0.27	25.63+0.45	72.53±0.48
F7	78.62+0.12	32.21±0.46	57.72+0.46
F8	81.66+0.56	27.49+0.35	52.54+0.57
F9	86.91+0.43	21.36+0.43	46.14±0.39
F10	73.33+0.42	34.10±0.33	53.42+0.28
F11	82.08+0.31	31.67+0.31	49.11+0.27
F12	83.75+0.48	26.37+0.28	39.04±0.44

All values represent mean±SD, n=3,

Abbreviation: PY-Percentage Yield, DL-Drug Loading, EE-Drug Loading

Table 3: Poly-dispersity index of formulated KPF-SLMs

Formulation code	PDI
F1	0.533±0.06
F4	0.270±0.07
F7	0.293±0.18
F10	0.297±0.03

All values represent mean±SD, n=3,

Abbreviations: PDI-Poly-dispersibility Index

Table 4: Correlation coefficient (*r*), reaction rate constants (*k*) and diffusion exponent (*n*) of the model equations applied to the release of drug from KPF-loaded SLMs

Formulation code	Zero order		First order		Higuchi		Korsmeyer-peppas	
	R^2	K_0	R^2	K_1	R^2	k_H	R^2	n
SLM1	0.796	4.3872	0.450	0.036	0.953	17.59	0.461	0.301
SLM 2	0.726	4.597	0.388	0.032	0.901	18.79	0.313	0.249
SLM 3	0.921	3.792	0.564	0.039	0.998	14.49	0.568	0.360
SLM 4	0.899	4.408	0.544	0.039	0.992	16.99	0.547	0.340

Table 5: *In-vitro* drug permeation profile investigated for marketed gel and SLM gel

Formulations	Cumulative release (µg/cm²)	Flux (µg/cm²/h)	Permeability coefficient (cm/h)
Marketed gel	61.43±0.53	252.4	10.09×10^{-4}
SLM-KPF-Gel	82.37±0.46	327.3	13.17×10^{-4}

All values represent mean±SD, n=3

Table 6: Anti-inflammatory activity of KPF-loaded SLMs and marketed gel formulation

Group	Anti-inflammatory activity	Time (h)							
		0	1	2	3	4	5	6	12
Control	Edema Rate %	0	52.63±4.2	58.81±3.80	63.41±7.06	66.12±7.41	58.21±4.73	52.14±4.88	46.16±4.33
Marketed Gel	Edema Rate %	0	27.21±3.46***	32.12±4.10***	37.00±5.12***	48.21±5.76***	43.12±6.11***	42.12±3.16**	40.10±2.95
	Inhibition Rate %	0	48.30	45.38	41.64	27.08	25.92	19.21	13.13
SLM-Gel	Edema Rate %	0	32.74±5.1***	34.76±2.40***	36.21±4.88***	37.10±4.29***	32.12±3.91***	29.27±4.66***	22.12±6.11***
	Inhibition Rate %	0	37.79	40.89	42.89	43.88	44.82	43.86	52.08

Values are the mean±SD of each group (n=3). Where '*' represents P values versus untreated control. All treated groups were simultaneously compared via one-way ANOVA. Where *** P<0.001 and **P<0.01.

Characterization of SLM Gel

KPF-loaded-SLMs Gel was prepared by dispersion method and prepared gel formulation was characterized for various physicochemical parameters as discussed below.

Homogeneity, pH, viscosity and spreadability

Developed gel was tested for homogeneity by visual inspection and was found clear without any kind of aggregation. The pH of prepared gel was found to lie at ~ 5.4±1.32 representing compatible with skin pH and acceptability for topical application [30]. In view point of patient's compliance, spreadability and extrudability of gel is considered as an important property which was also found to be appropriate. Spreadability was found to be 3.21+0.15 gcm/sec representing good spreadability. Viscosity is also an essential parameter as the release of drug from gel depends on viscosity. Obtained value of the viscosity was found to be 7188.43±16.7 cP and each value points represent as mean±S. D., n=3.

***In-vitro* permeation study of SLM Gel**

The optimized formulation F4 was further investigated for *In-vitro* rat skin permeability study. Comparative study was performed between marketed gel, used as standard and the developed gel (F4) which was approximately 2.5 % (marketed product composition). The permeability of drug was calculated by plotting graph between percent drug permeated against time (fig. 6). Higher permeation rate was observed for SLM-loaded-KPF gel i.e. more than 80% of drug permeated within 24h in comparison to marketed gel (fig. 6). Permeability parameters such as steady-state flux and permeability coefficient were also found significantly higher for developed gel formulation than the standard (table 5).

***In-vitro* anti-inflammatory activity**

In-vitro percent inhibition of albumin denaturation method was used to evaluate anti-inflammatory potential of SLM (fig. 7a). Results reveal that SLM-loaded-KPF Gel inhibited approximately 50 % of albumin denaturation within 2 h followed by steady sustained inhibition pattern (fig. 7a). This can be explained as a consequence of initial burst release of drug from microspheres followed by sustained release of drug from the particulate system. These results were better than those obtained for marketed drug which showed percent inhibition of 37% at 2 h. Likewise, from percent RBC membrane stabilisation assay (fig. 7b) it is clear that SLM-loaded-KPF gel was able to stabilize more than 50 % RBCs within 2 h and 70% membrane stabilization was achieved at 12 h in controlled manner. However marketed formulation results in 45 % of RBCs membrane stabilization observed at 2 h.

***In-vivo* anti-inflammatory study**

Further *In-vivo* anti-inflammatory study was carried out to reveal the effect of prepared gel formulation in animals through carrageenan induced rat paw edema model. Initially inhibition rate for developed gel was found to be 37.79 % as shown in table 6. Percent edema inhibition was found to be better for SLM-loaded-KPF Gel than marketed formulation. Throughout the study, inhibition rate was almost steady after 3h of drug application which can be explained in context to steady and sustained release of drug by 4h after an initial burst release. As sustained release is known to provide continues availability of drug to skin [31], here SLMs provides the sufficient surface area to facilitate contact of stratum corneum with drug, which ensure sustained release of the drug for longer duration of time. Empirically, high affinity is reported for *In-vivo* distribution of lipid particulate system inside the skin by no toxic effect and with non-irritant property [32].

CONCLUSION

Conclusively, KPF loaded microspheres were formulated and impact of different surfactants at various concentrations were studied. Microspheres were found to have optimum particle size and spherical surface morphology with respect to topical delivery. Physicochemical analysis suggested the successful incorporation of the poor water-soluble drug KPF with superior entrapment efficiency i.e. 82%. *In-vitro* and *In-vivo* anti-inflammatory studies represented faster onset of action and prolonged effect of KPF in comparison to marketed product. Therefore, this study not only confirms successful fabrication of SLMs but also provides a hint to utilize SLMs to overcome the bioavailability for poor water soluble drugs for topical/superficial infections.

CONFLICT OF INTERESTS

Authors declare no conflict of interest

ACKNOWLEDGEMENT

Authors would like to acknowledge Prof. (Dr.) P. K. Khosla (Vice chancellor, Shoolini University), Dr. Nitin Jain for their persistent assistance and for providing the facilities to carry out this project. Authors would also like to thank Himachal Pradesh University for the analysis of samples.

REFERENCES

1. Hooshmand H, Hashmi M, Phillips EM. Infrared thermal imaging as a tool in pain management-An 11 Y Study, Part I of II. Thermol Int 2001;11:117-29.

2. Davis CC, Squier CA, Lilly GE. Irritant contact stomatitis: a review of the condition. J Periodontol 1998;69:620-31.
3. Buckwalter JA, Lappin DR. The disproportionate impact of chronic arthralgia and arthritis among women. Clin Orthop Relat Res 2000;372:159-68.
4. Fiorucci S, Meli R, Bucci M, Cirino G. Dual inhibitors of cyclooxygenase and 5-lipoxygenase. A new avenue in anti-inflammatory therapy? Biochem Pharmacol 2001;62:1433-8.
5. Hersh EV, Lally ET, Moore PA. Update on cyclooxygenase inhibitors: has a third COX isoform entered the fray. Curr Med Res Opin 2005;21:1217-26.
6. Gertz M, Harrison A, Houston JB, Galetin A. Prediction of human intestinal first-pass metabolism of 25 CYP3A substrates from *in vitro* clearance and permeability data. Drug Metab Dispos 2010;38:1147-58.
7. Oates JA, Wood AJ, Brooks PM, Day RO. Nonsteroidal antiinflammatory drugs—differences and similarities. N Engl J Med 1991;324:1716-25.
8. Kantor TG. Ketoprofen: a review of its pharmacologic and clinical properties. Pharmacotherapy: J Human Pharmacol Drug Ther 1986;6:93-102.
9. Small G, Dubois B. A review of compliance to treatment in Alzheimer's disease: potential benefits of a transdermal patch. Curr Med Res Opinion 2007;23:2705-13.
10. Prausnitz MR, Langer R. Transdermal drug delivery. Nat Biotechnol 2008;26:1261-8.
11. Capan Y, Jiang G, Giovagnoli S, Na K-H, DeLuca PP. Preparation and characterization of poly (D, L-lactide-co-glycolide) microspheres for controlled release of human growth hormone. AAPS PharmSciTech 2003;4:147-56.
12. Jaspart S, Piel G, Delattre L, Evrard B. Solid lipid microparticles: formulation, preparation, characterisation, drug release and applications. Expert Opin Drug Delivery 2005;2:75-87.
13. Almeida AJ, Souto E. Solid lipid nanoparticles as a drug delivery system for peptides and proteins. Adv Drug Delivery Rev 2007;59:478-90.
14. Audu MM, Achile PA, Amaechi AA. Phospholipon 90G based SLMs Loaded with Ibuprofen: an oral anti-inflammatory and gastrointestinal sparing evaluation in rats. Pak J Zool 2012;44:1657-64.
15. MuÈller RH, MaÈder K, Gohla S. Solid lipid nanoparticles (SLN) for controlled drug delivery–a review of the state of the art. Eur J Pharm Biopharm 2000;50:161-77.
16. Sanna V, Kirschvink N, Gustin P, Gavini E, Roland I, Delattre L, *et al.* Preparation and *in vivo* toxicity study of solid lipid microparticles as carrier for pulmonary administration. AAPS PharmSciTech 2004;5:17-23.
17. Gavini E, Sanna V, Sharma R, Juliano C, Usai M, Marchetti M, *et al.* Solid lipid microparticles (SLM) containing juniper oil as anti-acne topical carriers: preliminary studies. Pharm Dev Technol 2005;10:479-87.
18. López A, Llinares F, Cortell C, Herraez M. Comparative enhancer effects of Span® 20 with Tween® 20 and Azone® on the *in vitro* percutaneous penetration of compounds with different lipophilicities. Int J Pharm 2000;202:133-40.
19. Reithmeier H, Herrmann J, Göpferich A. Lipid microparticles as a parenteral controlled release device for peptides. J Controlled Release 2001;73:339-50.
20. Higuchi T. Mechanism of sustained-action medication. Theoretical analysis of rate of release of solid drugs dispersed in solid matrices. J Pharm Sci 1963;52:1145-9.
21. Higuchi T. Rate of release of medicaments from ointment bases containing drugs in suspension. J Pharm Sci 1961;50:874-5.
22. Korsmeyer RW, Gurny R, Doelker E, Buri P, Peppas NA. Mechanisms of solute release from porous hydrophilic polymers. Int J Pharm 1983;15:25-35.
23. Sareen R, Kumar S, D Gupta G. Meloxicam carbopol-based gels: characterization and evaluation. Curr Drug Delivery 2011;8:407-15.
24. Patel D, Dasgupta S, Dey S, Ramani YR, Ray S, Mazumder B. Nanostructured lipid carriers (NLC)-based gel for the topical delivery of aceclofenac: preparation, characterization, and *in vivo* evaluation. Sci Pharm 2012;80:749.
25. Mizushima Y, Kobayashi M. Interaction of anti-inflammatory drugs with serum proteins, especially with some biologically active proteins. J Pharm Pharmacol 1968;20:169-73.
26. Asanuma M, Taguchi C, Kumagi T, Uesaka H, Hosokawa H, Kuriya S-i. The hydrogen ion concentration (pH) in blood samples with K2EDTA and K3EDTA affects mean corpuscular volume values in hemodialysis patients. Lab Hematol 2000;6:67-72.
27. Sadique J, Al-Rqobah W, Bughaith M, El-Gindy A. The bio-activity of certain medicinal plants on the stabilization of RBC membrane system. Fitoterapia 1989;60:525-32.
28. Gandhidasan R, Thamaraichelvan A, Baburaj S. Anti-inflammatory action of Lannea coromandelica by HRBC membrane stabilization. Fitoterapia 1991;62:81-3.
29. Nasr M, Mansour S, Mortada ND, El Shamy A. Lipospheres as carriers for topical delivery of aceclofenac: preparation, characterization and *in vivo* evaluation. AAPS PharmSciTech 2008;9:154-62.
30. Escribano E, Calpena AC, Queralt J, Obach R, Doménech J. Assessment of diclofenac permeation with different formulations: anti-inflammatory study of a selected formula. Eur J Pharm Sci 2003;19:203-10.
31. Paudel KS, Milewski M, Swadley CL, Brogden NK, Ghosh P, Stinchcomb AL. Challenges and opportunities in dermal/transdermal delivery. Ther Delivery 2010;1:109-31.
32. Mei Z, Chen H, Weng T, Yang Y, Yang X. Solid lipid nanoparticle and microemulsion for topical delivery of triptolide. Eur J Pharm Biopharm 2003;56:189-96.